Characterization of the H_2 sensing mechanism of Pd-promoted SnO_2 by XAS *in operando* conditions†

Olga V. Safonova,*[ac] Thomas Neisius,[a] Andrey Ryzhikov,[bc] Bernard Chenevier,[b] Aleksandre M. Gaskov[c] and Michel Labeau[b]

Received (in Cambridge, UK) 12th July 2005, Accepted 25th August 2005
First published as an Advance Article on the web 19th September 2005
DOI: 10.1039/b509826b

The effect of Pd nanoparticles on the H_2 sensitivity of SnO_2 thin films was studied in real working conditions using X-ray Absorption Spectroscopy (XAS), electrical conductivity measurements and mass-spectrometry.

Polycrystalline SnO_2 is the most popular material for the development of resistive gas sensors, which are used for the detection of toxic and explosive gases (CO, H_2, NO_x *etc*). SnO_2 is a wide band gap semiconductor of n-type. The sensor response is based on the fact that conductivity of this material depends on the atmosphere composition. Adsorption of oxygen on the SnO_2 surface creates so-called 'trapped charges'. Chemisorption and subsequent redox reactions of a target gas with the adsorbed oxygen species lead to modulations of the quantity of charge and a variation of conductivity. Deposition of metal nanoparticles (Pt, Pd) on the SnO_2 surface enhances the sensitivity to CO and H_2 and decreases the working temperature. However, the role of the nanoparticles in the sensor response process is still under discussion. Two mechanisms are mainly proposed: the 'chemical' and the 'electronic'.[1–5] The former is focused on the ability of the nanoparticles to dissociate oxygen, to spill over the SnO_2 surface and to catalyse the combustion of the target gas and even the reduction of the SnO_2 matrix.[6] The latter considers that conductance changes due to the variation of contact potential on the nanoparticle/SnO_2 interface caused by the change of the charge or the oxidation state of the nanoparticles.[5]

The aim of this work was to clarify the role of Pd in the H_2 sensing mechanism by measuring XAS at Pd K- and Sn L-edges simultaneously with the sensor properties *in operando* conditions.[7] Mass-spectrometry was also used *in situ* to quantify the amounts of H_2 and O_2, which participate in the reaction with the gas sensor material. To date, most of the studies on the reactivity of Pd nanoparticles on the SnO_2 surface were performed *ex situ* using XPS in UHV conditions,[3,5] which are not favourable since the gas sensor surface is extremely sensitive towards changes in atmospheric composition even at room temperature.[1] The main advantage of XAS is the possibility to probe directly the electronic states and local environments of Pd and Sn in the presence of a gas atmosphere (*i.e.* in real working conditions).

The gas sensing tests were conducted using an *in situ* cell (the picture is shown in ESI†) that allowed us to measure the XAS spectra and electrical conductance simultaneously. Pure and Pd-promoted (4.8 mol%) SnO_2 thin films (1.5 μm) were synthesized on polished alumina substrates by aerosol pyrolysis of metalloorganic precursor solutions.[8]‡ Samples were alternately exposed to 20% O_2 in He, 1000 ppm H_2 in He, and pure He (100 ml min^{-1} gas flow rate). The measurements were made at High Brilliance XAFS-XES beamline (ID26) at the ESRF. XAS spectra were collected in the florescence mode.§

The reversible increase of the electrical conductance of Pd–SnO_2 and SnO_2 films in the presence of H_2 is shown in Fig. 1. The amplitude of the conductivity variation is much greater for the film containing Pd. The absorption near Pd K-edge (24.3686 keV¶) was measured simultaneously with a time resolution of 1s. It is very interesting that considerable changes

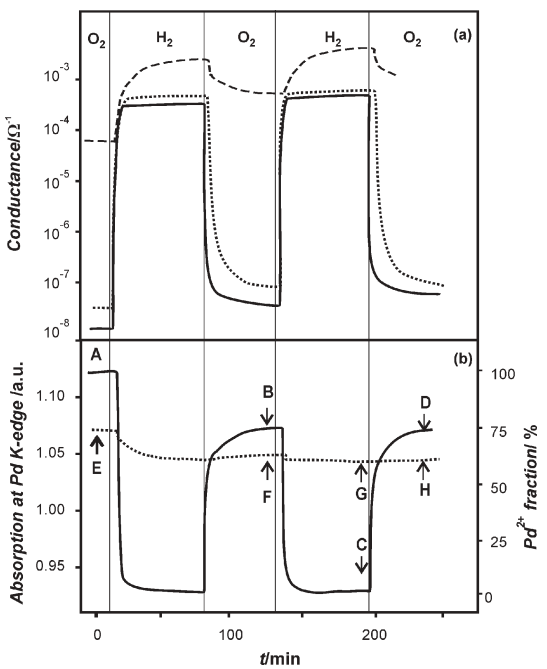

Fig. 1 Variation of the electrical conductance (a), normalized absorption at Pd K-edge (b, left scale) and Pd^{2+} fraction in the Pd^{2+}/Pd^0 mixture (b, right scale) for Pd–SnO_2 film at 573 K (solid lines) and 373 K (dotted lines) during the alternative exposure to 20% O_2 in He and 1000 ppm H_2 in He. The broken line corresponds to pure SnO_2 at 573K.

[a]*ESRF, PO Box 220, Grenoble Cedex, F-38043, France. E-mail: safonova@esrf.fr; Fax: +33(0)476882784; Tel: +33(0)476882922*
[b]*LMGP, CNRS UMR 5628, Institut National Polytechnique de Grenoble, BP 46, F-38402 Saint Martin d'Heres Cedex, France*
[c]*Chemistry Department, Moscow State University, Moscow 119992, Russia*

† Electronic supplementary information (ESI) available: Fig. 1: Photos of the *in situ* cell; Fig. 2: EXAFS spectra at Pd K-edge for Pd-promoted SnO_2 film; Table 1: Structural and statistical parameters for XANES and EXAFS spectra. See http://dx.doi.org/10.1039/b509826b

in the X-ray absorption that indicate oxidation and reduction of Pd particles take place only at higher temperature. In the steady-state conditions (A–H states on Fig. 1b) the full XAS scans (24.2–25.2 keV) were recorded. The same experiment was repeated to study the variation of tin oxidation state from XANES at Sn L-edges (3.9–4.5 keV).[9]

The XAS spectra were normalized and background corrected using IFFEFIT.[10] The factor analysis using ITFA_v1_3 software[11] singled out that normalized XANES spectra of Pd and Sn contain only two components. In order to quantify the Pd^{2+}/Pd^{0} and Sn^{2+}/Sn^{4+} ratios the linear combination analysis was performed using the same software.‖ Fig. 2 shows the examples of the fitted XANES spectra measured at Pd K- and Sn L1-edges for Pd-promoted SnO_2 in the steady-state conditions (A–H states are the same as in Fig. 1). For Pd EXAFS analysis the Fourier transformation was applied on the k^3–weighted $\chi(k)$ data in a typical k-range 3–13 $Å^{-1}$.** The examples of the fitted EXAFS spectra of Pd–SnO_2 analysis are given in the ESI†. It should be mentioned that EXAFS data analysis excludes the formation of a Pd hydride phase. The Pd–Pd distances in the samples are the same as in the Pd metal phase.

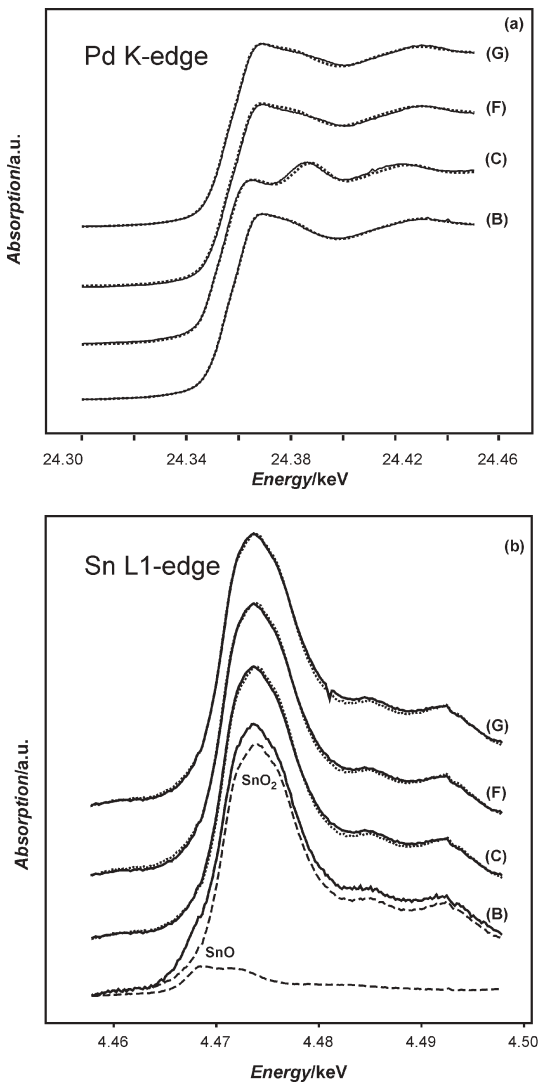

Fig. 2 The Pd K- (a) and Sn L_1 (b) spectra of Pd-promoted SnO_2. Solid lines—experimental data, dotted lines—the best fit, broken lines—deconvolution of the spectrum B.

Fig. 3 shows the correlation between the electrical conductance and the oxidation states of Pd and Sn during the cycling of Pd–SnO_2 film in H_2 and O_2 containing gas mixtures (the data points correspond to the second cycle in H_2 and O_2 as shown in Fig. 1). At 373K, the conductance changes without any variation of the Pd and Sn oxidation states. At higher temperatures, the mechanism becomes more complicated. The oxidation state of Pd varies considerably depending on the atmospheric composition. Pd nanoparticles also catalyse the reduction of SnO_2 matrix (formation of Sn^{2+} was not observed in the case of the pure SnO_2 film). However, there is no direct correlation between the conductance and the oxidation states of Pd and Sn. Fig. 3 shows that even at 573K the conductance of the Pd–SnO_2 film can change by several orders of magnitude *without any* measurable variation of the oxidation states of both metals. These results indicate that oxidation and reduction of Pd nanoparticles and SnO_2 matrix are the secondary processes, which are not responsible for the sensitivity to H_2. Moreover, the fact that Pd does not change its oxidation state mitigates against the 'electronic' mechanism, which explains the variation of the sensor response to the charge or the oxidation states of the nanoparticles,[5] as being responsible for the instantaneous change of the conductivity.

Further information about the chemical mechanism was obtained through analysis of mass-spectrometric data. To simplify the model we considered only three chemical processes:

$$O_{ads} + H_2 = H_2O \quad (1)$$

$$PdO + H_2 = Pd + H_2O \quad (2)$$

$$SnO_2 + H_2 = SnO + H_2O \quad (3)$$

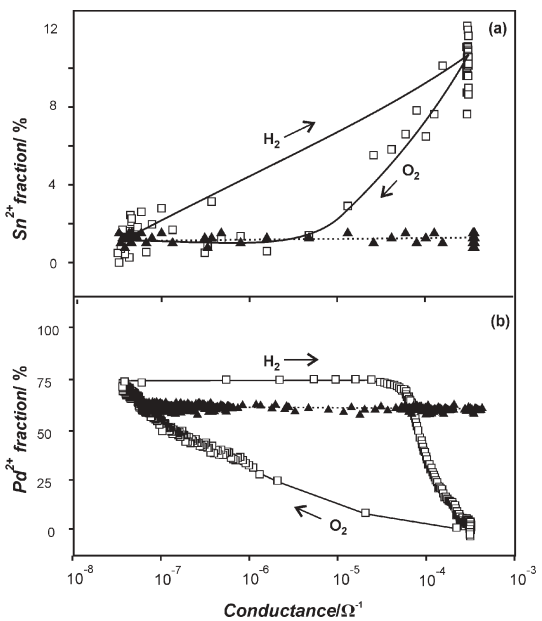

Fig. 3 The correlation between the conductance of Pd–SnO_2 film and the oxidation states of tin (a) and palladium (b) at 573K (white squares, solid lines) and 373K (black triangles, dotted lines). Fraction of Pd^{2+} is the concentration of Pd^{2+} in the Pd^{2+}/Pd^{0} mixtures; the fraction of Sn^{2+} is the concentration of Sn^{2+} in the Sn^{2+}/Sn^{4+}mixture. The arrows indicate the direction in which the system changes during exposure to H_2 and O_2

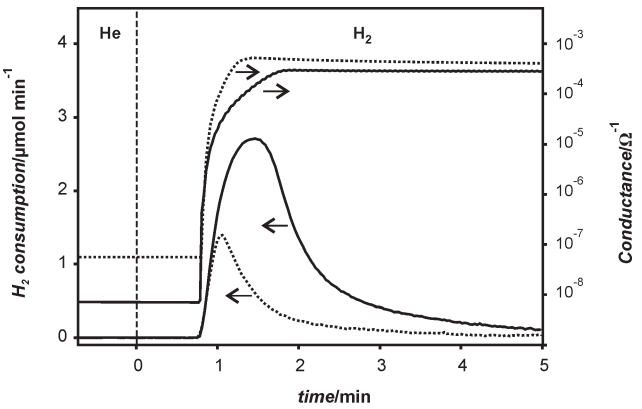

Fig. 4 The H_2 consumption rate and the conductance of the Pd–SnO_2 film at 573K (solid lines) and 373K (dotted lines).

Table 1 The parameters that characterize the reactivity of Pd–SnO_2 and pure SnO_2 films

Sample	T/K	$n[H_2]$/μmol[a]	n[SnO]/μmol[b]	n[Pd]/μmol[c]	a/ μmol[d]
Pd–SnO_2	573	3.7	1.43	0.74	1.53
Pd–SnO_2	373	1.1	<0.23	0.02	0.9[e]
SnO_2	573	0.26	<0.23	—	—
SnO_2	373	0.036	<0.23	—	—

[a] The total H_2 uptake; [b] The amount of SnO produced in reaction (3) (from XANES); [c] The amount of Pd produced in reaction (2) (from XANES); [d] $a = n[H_2] - n[SnO] - n[Pd]$. [e] This value is close to the one measured by Grass *et al.*[12] for Pt promoted SnO_2.

The samples were oxidized in 20% O_2 in He (1 h), then oxygen was purged by He (2 h), and, finally, a mixture of 1000 ppm H_2 in He was introduced into the cell. Pure alumina substrate was measured in the same conditions and used as a blank experiment. Fig. 4 shows that conductance of the Pd–SnO_2 film changes simultaneously with H_2 consumption.

The total uptake of H_2 calculated by the integration of H_2 consumption rate curves was found to be much greater for Pd-promoted than for pure SnO_2. Table 1 summarizes the results on the reactivity of the sensor films obtained independently from XANES and mass-spectrometry experiments.

Insofar as the weight of SnO_2 thin films is known (2.4×10^{-3} g), the amounts of Pd^0 and SnO produced in reactions (2) and (3) may be calculated from XANES data (see Table 1). According to our model, the difference between the total H_2 uptake and the amounts of Pd^0 and SnO and produced in the reactions (2) and (3) should correspond to the amounts of adsorbed oxygen participating in reaction (1) (*a* parameter in Table 1). Our measurements show that this value is much smaller for pure than for Pd-promoted SnO_2. This result indicates that Pd affects the chemical properties of the SnO_2 surface by enhancing the reactivity of adsorbed oxygen towards hydrogen. This can also be used to explain the role of Pd in the gas sensitivity mechanism that seems to be more 'chemical' than 'electronic'.

In conclusion, we have demonstrated how XAS, together with synchronous conductivity and mass-spectrometric measurements, can be applied to understand the mechanistics of gas sensing under dynamic operational conditions. The simultaneous use of these techniques permits delineation and clarification of how structural, electronic, and chemical phenomena interact to produce a functional material, in this case a Pd-promoted SnO_2 thin film gas sensor.

We gratefully acknowledge ESRF for provision of facilities at ID26 and ID24 (mass-spectrometer). Dr Mark Newton and Dr Pieter Glatzel are thanked for discussions and useful ideas. Dr Sergey Dorofeev and Christophe Lapras are also thanked for the development of the *in situ* set-up.

Notes and references

‡ Composition and microstructure of the films were studied by EPMA, XRD, SEM, TEM, STM, and AFM. Films have a porous structure and consist of 6–10 nm SnO_2 crystallites arranged into 100 nm agglomerates. The SnO_2 surface area is about 50 m^2g^{-1}. Pd is homogeneously distributed on the surface of SnO_2 crystallites.

§ The Pd K-edge XAS data was collected using 13-element Ge detector, tuned to Pd Kα fluorescence peak. To increase the signal-to-noise ratio the samples were measured at a small angle ($\sim 1^\circ$). An average of 2 scans was required with the scan time of 20 min. The XANES at Sn L_1, L_2 and L_3–edges was measured in normal geometry with Si diode using the continuous scan mode of the monochromator (30 s per spectrum).

¶ This energy corresponds to the maximum of PdO absorption.

‖ The Pd K-egde XANES spectra of completely oxidized (A) and reduced (C) Pd–SnO_2 were considered as pure components. In the case of tin the Sn L1-edge XANES spectra of pure SnO_2 and SnO were used for the same purpose.

** The data were analysed using phase shifts and amplitude functions of Pd-foil and PdO.

1 (*a*) G. Henshaw, R. Ridley and D. Williams, *J. Chem. Soc., Faraday Trans.*, 1996, **92**, 3411; (*b*) L. Moris and D. E. Williams, *J. Phys. Chem. B*, 2001, **105**, 7272.
2 S. C. Tsang, C. D. A. Bulpitt, P. C. H. Mitchell and A. J. Ramirez-Cuesta, *J. Phys. Chem. B*, 2001, **105**, 5737.
3 R. Cavicchi, V. Sukharev and S. Semancik, *Surf. Sci.*, 1998, **418**, L81.
4 M. Gaidi, J. L. Hazemann, I. Matko, B. Chenevier, M. Rumyantseva, A. Gaskov and M. Labeau, *J. Electochem. Soc.*, 2000, **147**, 3131.
5 M. Moroseac, T. Skala, K. Veltruska, V. Matolin and I. Matolinova, *Surf. Sci.*, 2004, **566–568**, 1118; T. Skala, K. Velttruska, M. Moroseac, I. Matolinova, A. Cirera and V. Matolin, *Surf. Sci.*, 2004, **566–568**, 1217.
6 (*a*) O. Safonova, I. Bezverkhy and Pavel Fabrichnyi, *J. Mater. Chem.*, 2002, **12**, 1174; (*b*) R. Sasikala and S. K. Kulshreshtha, *J. Therm. Anal. Calorim.*, 2004, **78**, 723.
7 (*a*) B. M. Weckhuysen, *Chem. Commun.*, 2002, 97; (*b*) B. M. Weckhuysen, *Phys. Chem. Chem. Phys.*, 2003, **5**, 4351.
8 O. V. Safonova, G. Delabouglise, B. Chenevier, A. M. Gaskov and M. Labeau, *Mater. Sci. Eng. C*, 2002, **21**, 105.
9 Z. Liu, K. Handa, K. Kaibuchi, Y. Tanaka and J. Kawai, *J. Electron Spectrosc. Rel. Phenom.*, 2004, **135**, 155–158.
10 A. L. Ankudinov, B. Ravel, J. J. Rehr and S. D. Conradson, *Phys. Rev. B*, 1998, **58**, 7565.
11 A. Roβberg, T. Reich and G. Bemhard, *Anal. Bioanal. Chem.*, 2003, **376**, 631.
12 K. Grass and H.-G. Lintz, *J. Catal.*, 1997, **172**, 446.